Peak Flow Prediction and Hydrologic Hazard Assessment for Kessem Dam by Using Machine Learning Models and RMC-RFA Software

Esayase Tesfaye Ergete
Arba Minch University
Elias Gebebeyhu Ayele (eliasg2000@gmail.com)
Arba Minch University

Research Article

Keywords: Kessem Dam, Peak Flow Prediction, Hydrologic Hazard Analysis, Dam Safety

Posted Date: June 22nd, 2022

DOI: https://doi.org/10.21203/rs.3.rs-1746769/v1

Abstract

In dam systems, flooding is a peak flow that the major problem and cause of dam failure in the form of overtopping phenomena, especially for embankment dams. A quantitative hydrologic risk assessment of the dam is used for dam safety evaluation in deciding whether existing structures provide adequate levels of safety, and if not, what modifications are justified to improve the dam's safety. This study considered the Kessem River watershed of the Awash basin, located at 9º8’45" latitude and 39º55'31" longitude at the southern end of the Afar rift in the Afar region of Ethiopia, and focused on the powerful method of prediction peak inflow to the reservoir, including the semi-quantitative assessment of hydrologic hazard for Kessem Dam using machine learning predictive models and RMC-RFA software. The most recent three RNN (LSTM, Bi-LSTM, and GRU) machine learning predictive models with hybrid to SCS-CN model were used for simulation of Kessem river flow. Peak daily inflow events to the reservoir are predicted to be 467.72 m^3/s, 435.88 m^3/s and 513.55 m^3/s in 2035, 2061, and 2090, respectively. The hydrologic hazard analysis results show that 2,823.57 m^3/s and 935.21 m, 2,126.3 m^3/s and 934.18 m, and 11,491.1 m^3/s and 942.11 m peak discharge and maximum reservoir water level during the periods of 2022–2050, 2051–2075, and 2076–2100, respectively, for 0.0001 APE. As concluded, Kessem dam may potentially be overtopped by a flood with a return period of about 10,000 years during the period of 2076–2100. So, the dam required further risk analysis study and dam safety modification in order to control this probable failure mode during the indicated time.

1. Introduction

A flood is the most dangerous natural disaster in the world in various areas year after year, caused by peak runoff from the river during a period of extremely high precipitation and creating destruction in inundation areas (Getahun and Gebre 2015; Khalaf et al. 2018; Subramanya 2008). Floods have occurred in various areas of Ethiopia for several years (Assefa 2018; OCHA 2020). In particular, in July 2017, a flash flood overwhelmed Meteka town in Ethiopia's Afar region, which was a dangerous flood. It was a near-year event that resulted in the displacement of many people (OCHA 2020; Shumie 2019). This flood inundation area is located downstream of the study area (Shumie 2019). The main causes of this disaster are an unexpected peak flow in that area, which is possibly one of the main causes of its occurrence, are dam overtopping and excess water surplus from the reservoir. These flood events are a series of problems in the lowlands of our country of Ethiopia, especially in the Awash basin (Getahun and Gebre 2015), with its values changing due to increased human activities within the river system, climate change, and changes in land use land cover for the upstream part of the watershed, which also leads to a change in watershed character (Mahmood et al. 2010; Sivapalan et al. 2005; Vo et al. 2015).

Flooding can cause major problems for people living close to the river (Raghunath 2006), and raising the water level in the reservoir is the main cause of dam failure due to overtopping, especially for embankment dams. The erosive action of water flow during overtopping is the primary cause of dam body failure (Jandora and Riha 2008). To effectively control and reduce the effects of these events, the frequency and magnitude of peak flow should be predicted using advanced techniques (Le et al. 2019).

Dam failures mostly occur due to overtopping. The main cause of dam overtopping and river channel overflow is peak flow occurring in the watershed which increases the reservoir as well as river channel water level. For instance; The South Fork Dam, also known as Johnstown Dam (the 72-foot-high dam was an earth fill embankment located in western Pennsylvania in United State) dam failed on May 31, 1889, due to overtopping failure during a large flood, the Secondary Dam of Sella Zerbino (a dam that were competed in 1925 to form a reservoir on the Orba River, in South Piedmont, Italy) failed as a result of the overtopping on August 13, 1935, Gibson Dam (a 199-foot-high concrete arch dam constructed by Reclamation on the Sun River on the east side of the Continental Divide in Montana) about 3.2 feet of a maximum overtopping was occurred on June 8,1964 due to a major flood developed in the area, Teton Dam (located in southeastern Idaho, Washington) failed on June 5, 1976 and Tous dam (a 70 m high rock fill dam with a central clay core located near Valencia, Spain) failed due to overtopping on October 19, 1982 (Sharma and Ali 2013). Therefore, to avoid or reduce this phenomenon by taking flood control measures in a watershed and provide sufficient emergency spillway (diversion floodway) and others dam safety modification for minimizing the dam safety risk (Adamo et al. 2017; Adiel et al. 2015; Herrero and Garrote 2020; Mcgrath 2000; Mo et al. 2018; Rao and Hamed 2000). In the study area, According to Shumie (2019) study, he provided the best structure like a diversion floodway to control floods and to save the dam from overtopping and failure. However, the gap of the previous study in the Kessem watershed is did not properly predict future peak flow and did not analyze and assess risk in the watershed as well as for dam.

Moreover, machine learning models are the most powerful and latest predictive models in water systems by using the concept of data-driven techniques (Hosseiny et al. 2020; Mich 2020). That means the machine learning models establish the relationship between input and output based on data driving techniques and contain no physical transformation function to relate input to output. Machine learning models are one of the most simple, powerful, and robust models for mapping the non-linear relationship between rainfall and runoff, even though they cannot represent the physical process of the catchment (Kratzert et al. 2018). Thus, sometimes data-driven models do not give better results as the underlying physical processes have been ignored in the model. This is because the amount of runoff variance can be based on antecedent moisture content (AMC) and physical characteristics of the catchment such as geology, soil, slope, and land use/land cover (LULC) conditions (Mahmood et al. 2010). Therefore, the main constraint of machine learning for hydrological models is the non-consideration of physical processes, so this study used a hybrid it with the physically based (SCS-CN) models (it’s able to represent the spatial variability of land surface characteristics such as LULC and soil type) in order to increase the machine learning model’s performance for prediction of peak flow. Therefore, the main objective of this study is to forecast the peak flow to Kessem reservoir by using selected Machine Learning model and integrate it to RMC-RFA for hydrologic hazard analysis and assessment for Kessem dam in Awash basin, Ethiopia.

2. Materials Used And Methodology

2.1 Description of the Study Area

The awash basin is one of a major Ethiopian basin, Kessem river is the most tributary to this basin at the middle section which southern end of the Afar rift in the Afar regional state of Ethiopia, 225 km east of Addis Ababa and 40 km northwest of Metehara town and constructed on it Kessem dam located at 9^{o}8’45” Latitude and 39^{o}55'31" Longitude for storage half-billion cubic meter capacity of the reservoir to supply the irrigation demand for irrigated areas of 20,000 ha at lower of Kessem dam irrigation project. The following Fig. 1 shows the topographic map of the study area.

2.2 Data Collection

Data availability is a critical and crucial requirement for conducting any research. It is impossible to produce a justified outcome without reliable data and information. To produce accurate and sensible outcomes, processing necessitates a collection of data and information. As a consequence, data should be gathered from many sources and institutions. Hydro-meteorological data (Stream flow data, precipitation and temperature data), a digital elevation model, land used/cover and soil type map data were collected for this study in order to predict a flood amount and assessment of the risk on dam safety.

Daily precipitation (in the form of rainfall) data from 1988-2018 years of 15 stations around and in the Kessem watershed were collected from Ethiopian meteorological agency. However, 11 rainfall stations were selected for this study based on the availability and continuity of data and more that contribute to the Kessem River. And others Climate data such as maximum and minimum temperature for six stations were collected from Ethiopian Meteorological Agency. Twenty-one years from 1990 to 2009 and four years from 2010 to 2013 of daily stream flow data for the Kessem River at Aware Melka and Kessem dam stations, respectively, were gathered from the Ministry of water and energy (MoWE) Hydrology Department. There were some breaks and missing parts of the collected data in the time series. Recorded water levels for Kessem reservoir from 2018 to 2021 were collected from the Ethiopian Construction Works Cooperation (ECWC) dam and irrigation development center.

A Digital Elevation Model (DEM) is a regular array of z values that a numerical representation of terrain elevation that contains coordinates and accompanying elevation values in a grid format. For this study, 1 arc second (30 m*30 m) resolution ASTER GDEM (Advanced Space borne Thermal Emission and Reflection Radiometer Global-DEM) downloaded from United States Geological Survey (USGS) earth Explorer data on website of (https://earthexplorer.usgs.gov/) for the shape of the Awash basin was collected from the MoWE GIS Department, then the Kessem sub-basins of the middle part of Awash were extracted from Awash DEM by following the procedural steps of watershed processing and used it for further analysis. The following Fig. 2 shows the hydro-meteorological stations of the study area.

2.3 Material Used

The following open source software was used extensively in this study. ArcGIS (geographical information system) software to analysis spatial data, selected models from AI/machine learning models for prediction of a flow/flood, Statistical Downscale Model version of SDSM 4.2.9 (Wilby and Dawson 2007) to

downscale climate information from coarse-resolution of GCMs to local or site level, Python 3.9 for the programming language (Rossum 1995) within the Jupyter notebook for writing and running the code, Matplotlib (Hunter 2007) for data visualization, hydrostats packages for evaluation of model performance (Roberts et al. 2018), RMC-RFA software for reservoir routing and analysis of hydrologic hazard on dam, SFE_IFC MATLAB toolbox to determine the flood characteristics (start and end date, peak and duration) and to develop flood hydrograph (Zhang et al. 2021) and Hydrological Engineering Center-Statistical Software Packages (HEC-SSP 2.2) software for volume-frequency analysis for Kessem Dam(Bartles et al. 2019).

2.4 Methodology

The observed climate data and flow that used to calibrate and validate the selected models have been collected from National meteorological service agency of Ethiopian and ministry of water and energy. DEM data and Landsat images were used as input for reclassified LULC approach processed by Arc GIS, Arc hydro tools for the catchment delineation and estimation of catchment characteristics.

The course climate data (GCM) that downloaded from the Canadian Climate Data and Scenarios (CCDS) portal CanESM2 model outputs for the study area are downscaled into finer spatial resolution at watershed level by bias correction through SDSM statistical approach and by using the selected potential predictors projected the future climate (precipitation and temperature). The Landsat images with different bands downloaded from USGS earth explore data for the study area and reclassified the LULC class in watershed used supervised classification techniques. The climate projected data under climate change scenario and LULC used as input for the SCS-CN model to estimated runoff at each sub watershed outlet. The output of SCS-CN model used as input of ML models to predict flow at Kessem dam watershed outlet and estimated flood event within future three-time horizons. Then import the results to RMC-RFA software to assess future hydrological risk of the selected flood events on Kessem reservoir for dam safety evaluation.

3. Results And Discussions

3.1 Climate Projection and LULC Changes

3.1.1 Climate Projection at the Future

The climate data (temperature and precipitation) projection at future within the watershed have been studied using CanESM2 climate model for RCP2.6, RCP4.5, and RCP8.5climate scenarios from coupled model inter-comparison project 5 (CMIP5) experiments which have been downscaled by statistical downscaling model (SDSM).

After trial and error to get the highest model performance by changing the values of bias correction and variance inflation in the SDSM model for precipitation, maximum temperature, and minimum temperature, the statistical results are as shown in the Table 1 to 3 below, and the mean values of the graphical results

are shown in Fig. 3 to 5 for each predictand. The selected potential predictors for calibrating the model were ncepp8_ugl, ncepp8_thgl, nceps500gl, ncepshumgl, and nceptempgl, with 1.356 bias correction and 12 value of variance inflation for precipitation, ncepp1_ugl, ncepp1thgl, nceps500gl, nceps850gl, ncepshumgl, and nceptempgl predictors with the values of bias correction and variance inflation of 1 and 12 respectively, were used for the model calibrated for minimum temperature, and nceps500gl, nceps500gl. ncepp1_zgl, ncepp5_fgl, ncepp5_vgl, ncepp500gl, ncepp5thgl, ncepp8_vgl, ncepp8_zgl, and nceptempgl predictors with the values of bias correction and variance inflation of 1 and 12 respectively were used for model calibrating, validating, and testing for maximum temperature.

Table 1
The performance results from SDSM model for downscaled precipitation after taken different trial and erro

Period		RMSE	NSE	R
Calibration		3.795	0.319	0.584
Validation		1.529	0.309	0.597
Testing	**RCP8.5**	3.446	0.324	0.625
	RCP4.5	3.429	0.331	0.613
	RCP2.6	3.371	0.353	0.601

After calibrated and validated the model, statistical evaluated values of RMSE, NSE and R were 3.446, 0.324 and 0.625, 3.429, 0.331 and 0.613, 3.371, 0.353 and 0.601 respectively for model performance to downscaled precipitation during testing period under RCP 8.5, RCP 4.5 and RCP 2.6 climate scenario respectively, from analysis, the SDS model was super performed during testing period under RCP2.6 climate scenario to downscaled precipitation, however, this scenario used to project the precipitation data at future time horizons from 2022 to 2050, 2051 to 2075 and 2076 to 2100 in Kessem watershed.

Table 2
The performance results of SDSM model for downscaled minimum temperature after taken different trial and error

Period		RMSE	NSE	R
Calibration		1.586	0.509	0.722
Validation		1.514	0.582	0.779
Testing	**RCP8.5**	1.722	0.312	0.662
	RCP4.5	1.697	0.332	0.670
	RCP2.6	1.678	0.346	0.676

After calibrated and validated the model, statistical evaluated values of RMSE, NSE and R were 1.722, 0.312 and 0.662 respectively under RCP 8.5, 1.697, 0.332, and 0.670 respectively under RCP 4.5, 1.678, 0.346, and 0.676 respectively under RCP 2.6 climate scenario (Table 2) for that indicate the model performance to downscaled minimum temperature during testing period. From analysis, the SDS model was super performed during testing period also under RCP2.6 climate scenario to downscaled minimum temperature, however, this scenario used to project the minimum temperature data at future time horizons from 2022 to 2050, 2051 to 2075 and 2076 to 2100 in Kessem watershed.

Table 3
The performance results from SDSM model for downscaled maximum temperature after taken different trial and error

Period		RMSE	NSE	R
Calibration		1.265	0.489	0.715
Validation		1.179	0.522	0.780
Testing	**RCP 8.5**	1.443	0.114	0.624
	RCP 4.5	1.418	0.144	0.646
	RCP 2.6	1.429	0.129	0.628

After calibrated and validated the model, statistical evaluated values of RMSE, NSE and R were 1.443, 0.114, and 0.624 respectively under RCP 8.5, 1.418, 0.144, and 0.646 respectively under RCP 4.5, 1.429, 0.129, and 0.628 respectively under RCP 2.6 climate scenario (Table 3) for the model performance of downscaled maximum temperature during testing period. From analysis, the SDS model was super performed during testing period under RCP 4.5 climate scenario to downscaled maximum temperature in this study area, therefore, this scenario used to project the maximum temperature data at future time horizons from 2022 to 2050, 2051 to 2075 and 2076 to 2100 in Kessem watershed.

3.1.2 LULC Changes and Scenario at the Future

Analysis of Land Used Land Cover (LULC) map in ArcGIS 10.5 by using the Landsat 8 and Landsat 7 images that download from USGS for path 168, row 54 with different bands at different acquired years (at 2000, 2010, 2020). Reclassified the download images by using supervised classification method to seven different LULC types namely, Agricultural lands, Bare Lands, Forests Areas, Grass Lands, Settlement's Areas, Shrub Lands, and Water Bodies for each acquired year by helping ArcMap 10.5 GIS software show as below Fig. 6.

Based on the collected sample data confusion matrix is as shown in Table 4. The total sample points (TS) are 71, and the total corrected classified (TCS) values is 57, the sum of the product values in the total ground truth column and in the total user row is 1101. Then, substituting those values in to the following Eqs. (1) and (2), the overall accuracy and kappa coefficient are 80.3 percent and 0.75, respectively. This means that 80.3 percent of land use and land cover classes are correctly classified.

$$Overall Accuracy(\%) = \frac{Total Number of Correctly Classified Pixels(Digonal)}{Total Number of \text{Re}ference(Ground Truth) Pixels} * 100 \quad \ldots\ldots\ldots\ldots\ldots\ldots (1)$$

$$Kappa Coefficient(K) = \frac{(TS * TCS) - \sum (Column Total * Row Total)}{TS^2 - \sum (Column Total * Row Total)} \quad \ldots\ldots\ldots\ldots\ldots\ldots\ldots\ldots (2)$$

Table 4
Create confusion matrix based the collected sample of ground truth and user classified in Kessem watershed

Class name	AG	BL	F	GL	S	SL	WB	TGT
AG	25	0	1	0	0	1	0	27
BL	0	1	0	3	0	1	0	5
F	0	0	7	0	0	1	0	8
GL	2	0	2	3	1	0	0	8
S	0	0	0	0	6	0	0	6
SL	0	0	1	1	0	10	0	12
WB	0	0	0	0	0	0	5	5
TUC	27	1	11	7	7	13	5	71
Total samples (TS)					71			
Total corrected classified (TCS)					57			
Overall Accuracy (%)					80.3			
Kappa Coefficient (K)					0.75			
Note: *TGT-Total ground truth and TUC- Total user classified*								

A LULC change detection study was performed by the supervised classification method using the maximum likelihood classifier algorithm in ArcGIS 10.5 software during the period 2000 to 2020. Table 5 shows the changing area covering of each LULC class in Kessem watershed for past 20 years.

Table 5
LULC changing in Kessem Dam watershed from 2000 to 2020

Class Name	Areas Cover at 2000 (km^2)	Areas Cover at 2010 (km^2)	Areas Cover at 2020 (km^2)	Change in %/year 2000–2010	Change in %/year 2010–2020	Change in %/year 2000–2020
AG	422.3	541.23	795.97	2.82	4.71	4.42
BL	16.46	15.681	12.414	-0.47	-2.08	-1.23
F	613.6	455.23	540.33	-2.58	1.87	-0.60
GL	241.6	219.87	55.768	-0.90	-7.46	-3.85
S	68.97	80.380	93.197	1.65	1.59	1.76
SL	1614.6	1664.6	1432.9	0.31	-1.39	-0.56
WB	0.004	0.516	46.926	14.24	8.99	6.52

Quantitative analysis of the overall LULC changes as well as decreases and increases in each class between 2000 and 2020 were gathered. The result as shown in Table 5 from the analysis, considerable decreases in Forest (0.6%), grass land (3.85%) and bare land area (1.23%) and shrub lands (0.56%) per year were observed during this period. On the other hand, increases in Agriculture lands (4.42%), settlement areas (1.76%) and surface water bodies (6.52%) for the same time period were also detected. Based on the analysis, the future LULC change scenarios in the Kessem watershed for each class were decided as follows.

Scenario 1: Forest, bare lands and shrub lands area have been reduced and all Grass land areas were covered by Agriculture lands, settlement areas and surface water bodies during the period 2022–2050.

Scenario 2: Under this scenario, further reductions have been made in forest, bare lands and shrub lands area for the period 2051–2075. These were then covered by Agriculture lands, settlement areas and surface water bodies.

Scenario 3: Under this scenario, reduction has been made on area covered by agriculture lands resulting in the formation of bare land for the period 2076–2100 and in addition to the condition made reduction in forest and shrub lands area were increases in settlement area and surface water bodies.

3.2 Flow/ Peak Flow Prediction at the Future Time Horizons

In ML model, the effective rainfall, potential evapotranspiration (Mahmood et al. 2010) and Stream flow data are the main input datasets that were used. All these datasets used are observation data and estimated data based on observation to calibrate and validated the models.

The effective rainfall was estimated by using SCS-CN model with considering the characteristics of sub-watershed of Kessem River. The PET was also computed used by Hargreaves methods based on the observed maximum and minimum temperature data at each available station in Kessem. The complete

stream flow data for Kessem River at Kessem Dam during the observed period of 1990–2013 were the transformed data by using area ratio transform techniques from Aware Melka station to Kessem dam during the period of 1990–2009 and the observed stream flow at Kessem dam during the period of 2010–2013. Based on the climate projection data and LULC scenario future flow was predicted by using the performed ML models with hybrid SCS-CN model.

Daily time series data have been used in the present study. The model was constructed using Keral Tensor Flow packages in python 3. Training and testing were performed for the period 1990 to 2013, for which observed discharge data are available. In the network modeling, out of the total data, 70% (January, 1990 - October, 2006) were selected for training and 30% (November, 2006 –December, 2013) each for testing.

In this study, implement three different deep learning methods (LSTM, Bi-LSTM, GRU) for flow prediction during the historical period. After trained the prediction models applied to predict flow for calibration and validation period, and then their performance is measured. Daily stream flow to the Kessem Dam reservoir in Kessem watershed was simulated using various deep-learning models. In this section, the historical observation stream flow data are compared with the computed stream flow from RNN models, such as LSTM, Bi-LSTM, and GRU using thirty lag days. A network attempts to predict outcomes as accurately as possible. The value of this precision in the network is obtained by the cost function, which tries to penalize the network when it fails. The optimal output is the one with the lowest cost. In this study, for the applied networks of Mean Square Error (Shoaib et al. 2014), the cost function is used. A repetition step in training generally works with a division of training data named a batch size. The number of samples for each batch is a hyper parameter, which is normally obtained by trial and error. In this study, the value of this parameter in all models is 128 in the best mode. In each repetition step, the cost function is computed as the mean MSE of these 128 samples of observed and predicted stream flow. The number of iteration steps for neural networks is named an epoch; in each epoch, the stream flow time series is simulated by the network once. Like other networks, neurons or network layers can be selected arbitrarily in recurrent networks. For the purpose of the comparison of models with each other, the structures of all recurrent network models are created identically. In each network, a double hidden layer is used so that there are 12 units in each the first layer and the second layer. The last layer output of the network at the final time step is linked to a dense layer with a single output neuron. Between the layers, a dropout equal to 10% is used. The structure of the neural network is also used in two hidden layers. The first and second layers have 12 neurons for each. In all networks, the sigmoid activation function is applied for the hidden layer. The main advantage of using sigmoid is that, for all inputs greater than 0, there is a fixed derivative. This constant derivative speeds up network learning. Each method is run with different epoch numbers. After taken different trial and error, the optimal hyper-parameter networks as shown in Table 6.

Table 6
Optimal hyper-parameter networks

Hyper-parameter	Values
Neuron	12
Optimization	Adam
Learning rate	0.001
Activation function	Sigmoid and Tanh
Max Epoch	4000
Batch size	128

The optimized model results were evaluated using Hydrostats packages with statistical error assessment techniques. In Hydrostats, the statistical as well as graphical evaluations are made using error metrics function between observed and simulated flow. Graphically by plotting the predicting and observed flow (Fig. 7), and several descriptive statistics can be used for evaluation of predictive models. In this study, RMSE, NSE, R^2 have been purposively used, and the results of different methods based on the evaluation criteria are presented in Table 7. Among the RNN methods, Bi-LSTM is super performed.

Table 7
Statistics evaluation of the model's performance of proposed ML models

ML Models	Training Period (1990–2006)				Testing (2006–2013)			
	RMSE	NSE	R^2	KGE	RMSE	NSE	R^2	KGE
BiLSTM	3.873	0.968	0.994	0.702	17.547	0.744	0.749	0.832
LSTM	4.276	0.962	0.974	0.777	19.878	0.672	0.727	0.690
GRU	4.003	0.966	0.982	0.743	20.703	0.644	0.681	0.712

The calculated discharges match well with the observed, as indicated by the high NSE and the small RMSE values for the overall evaluation of three ML models reveals that the Bi-LSTM models outperform than LSTM and GRU. Therefore, in this study the result of Bi-LSTM model to predict the flow of Kessem River at Kessem dam within three-time horizons is used.

3.3 Hydrologic Hazard Analysis for Kessem Dam

3.3.1 Inflow Hydrograph Shape

From 2022–2100 years of the future period of inflow to Kessem Dam, the selected three events on September 2035 from 2022–2050-time horizon, September 2061 from 2051–2075-time horizon and September 2090 from time horizon of 2076–2100 are the largest peak flow events that will have been occur in the Kessem dam watershed within the next 100 years.

Inflow hydrograph shapes for the three-time horizons shown in Fig. 8 that were derived using the results from the predicted ML model, The September 2035, September 2061, and September 2090 events were used for rescaling the sampled inflow flood events.

Moreover, the PMF hydrograph was developed based on 9237 m^3/s (Qp) of the design of the peak inflow PMF for a 10,000-year return period of Kessem dam by using SCS dimensionless methods with a time to peak (Tp) of 33.39 hours, including the watershed characteristics (L = 136.64 km = 448,294 ft, Sl = 1.238%, CN = 79.41 and Tc = 51.016 hours) to compute discharge Q and the corresponding time t. as shown in Fig. 9, which depicts the PMF hydrograph that plot the computed value of discharge Q versus time t.

This hydrograph was used in this study to compare with the results of peak discharge and stage frequency from hydrologic hazard analysis and to determine whether future flood events on the Kessem dam are at risk or not.

3.3.2 Inflow-Volume Frequency Curve

The developed volume-frequency curve of Kessem dam (Fig. 10) are based on the Log Pearson Type III distribution with a mean, a standard deviation, a skew coefficient and the effective record length values for the future within three-time horizons. For the volume frequency analysis, the Bulletin 17C with EMA analysis was performed using HEC-SSP, the resulting population moment estimates are shown in Table 8.

Table 8
The result of statistics from volume frequency analysis for each future time horizons

Period/Statistics	mean (of log)	standard deviation (of log)	skew (of log)	effective record length
2022–2050	2.446	0.125	0.654	29
2051–2075	2.375	0.107	0.450	25
2076–2100	2.461	0.174	1.087	25

Based on the result of volume frquency analysis, then compute the volume frequency curve with in 90% uncertainty bounds for Kessem dam for each of the corresponding future time horizons as shown as Fig. 10.

3.3.3 Flood Seasonality Analysis

For the threshold value of 206.4m^3/s, the frequency sample size during the period of 2022–2050, 2051–2075 and 2076–2100 is 35, 31, and 37 respectively; those are adequate sample size to analysis the flood seasonality for each time horizons. The flood seasonality histogram developed for this analysis for each timeframe can be seen below in Fig. 11. As results of this analysis, the annual flows normally flow from October through May, with June-September as the wettest months but flood seasonal month is August during the period of 2022–2050, while the annual flows normally flow from November through June, with July-October as the wettest months but flood seasonal month is September for each during the period of 2051–2075 and 2076–2100.

3.3.4 Reservoir Starting-Stage Duration Analysis

Initial reservoir levels and associated exceedance probabilities should be estimated from daily reservoir elevation estimates for the period of record at Kessem dam. Looking at the duration curve results below indicate that a median reservoir elevation for the June through October period is approximately 926 m, with a quartile range (25 to 75 percentiles) from about 922 to 928 m (Fig. 12), This reservoir elevation range should be considered as initial reservoir water surface elevations for routing the hydrographs. From the results and also will notice that August produces the lowest pool duration curve. This is important because as saw in the flood seasonality analysis section, floods are most likely to occur in August and September. However, the dam is operated with consideration of this flood seasonality. Therefore, large events are most likely to occur in August and September, but they are also most likely to have low reservoir starting pools, mitigating some of the risk for large peak stage events in the summer season.

3.3.5 Hydrologic Hazard Curve for Kessem Dam

When RMC-RFA finishes computing, it will automatically create the Stage-Frequency Curve and Hydrologic Hazard Curve plots as shown in Figs. 13 and 14respectively. The median curve represents the uncertainty in stage frequency and peak discharge frequency due to natural variability. The 95% uncertainty bounds represent the uncertainty in stage and peak discharge frequency due to knowledge uncertainty, whereas the expected curve represents the combined uncertainty due to both natural variability and knowledge uncertainty. Those curves are used for semi-quantitative risk analysis for Kessem dam.

From HHA (Figs. 13 & 14) produces the expected peak discharge and the corresponding peak stage for 100 to 1,000,000 year of return period for each time horizons see in Tables 9 and 10, respectively.

Table 9

Expected probable peak discharge (m^3/s) for each future time horizons

Return period	2022–2050		2051–2075		2076–2100	
	Expected	95% Bounds	Expected	95% Bounds	Expected	95% Bounds
100	867.67	669.3–1168	809.4	621–1082	1,230.9	759-2,308
1000	1,383.95	835-2294.8	1,178.9	705–1796	2,770.7	1,003–8,013
10,000	2,823.57	987-5430.6	2,126.3	790–3468	11,491.1	1,357 – 17,217
100,000	5,686.2	1,115 – 10,429.3	3,738.5	851–5811	17,292.3	1,636 – 17,726
1,000,000	12,916.72	1,147 – 15,231.7	7,104.67	887–9625	17,733.7	1,900 – 17,777

Table 10
Expected probable peak stage (m) for each future time horizon

Return period	2022–2050		2051–2075		2076–2100	
	Expected	95% Bounds	Expected	95% Bounds	Expected	95% Bounds
100	931.92	931.4-932.6	931.77	931.2-932.4	932.7	931.6-934.5
1000	932.94	931.7-934.5	932.54	931.5-933.7	935.13	932.2-940.9
10,000	935.21	932.1-938.4	934.18	931.7-936.1	942.11	932.8–943
100,000	938.59	932.2-941.8	936.37	931.8-938.7	943	933.3–943
1,000,000	942.42	932.4–943	940.1	931.9-941.6	943	933.7–943

Kessem Dam has a spillway discharge capacity of 6180 m^3/s at the maximum water surface elevation of 939.5 m. Comparing this value with the stage and peak discharge frequency curve indicates that the spillway is capable of passing a flood with a return period of 100–100,000 years for the future time horizons (2022–2075).

During the period of 2022–2050, the expected peak discharge for a 1/10000 AEP was equal to 2,823.57 m^3/s. The 10,000-year peak discharge at 95% confidence upper and lower limits is 987 m^3/s and 5,430.6 m^3/s, respectively, from the hydrological hazard analysis. The corresponding expected peak stage for 0.0001APE is 935.21 m, and the lower and upper 95% of bounds values are 932.1 m and 938.4 m, respectively. it is not exceeded the PMF discharge of 6180 m^3/s and the maximum water surface elevation of 939.5 m.

During the period of 2051–2075, the expected peak discharge for a 1/10000 AEP is equal to 2,126.3 m^3/s. The peak discharge at 95% confidence upper and lower limits is 790 m^3/s and 3468 m^3/s, respectively (Table 4.9). The corresponding peak stage for expected value and 95 percent lower and upper bounds values of 0.0001 APE is 934.18 m, 931.7m, and 936.1 m, respectively. The PMF discharge of 6180 m^3/s and maximum water surface elevation of 939.5 m are also not exceeded by those values.

During the period of 2076–2100, the expected peak discharge for a 1/10000 AEP was equal to 11,491.1 m^3/s. The 10,000-year peak discharge at 95% confidence upper and lower limits is 1,357 m^3/s and 17,217 m^3/s, respectively, from the hydrological hazard analysis. The corresponding expected peak stage for 0.0001APE is 942.11 m, and the lower and upper 95% of bounds values are 932.8 m and 943 m, respectively. It is exceeded that from the PMF discharge of 6180 m^3/s and the maximum water surface elevation of 939.5 m.

The results from this initial hydrologic hazard curve characterization and flood hydrograph routing indicate that Kessem dam may potentially be overtopped by a flood with a return period of about 10,000 years during the period of 2076–2100. However, this indicates that Kessem Dam does not meet Reclamation hydrologic hazard criteria for overtopping because it does not pass through a PMF for 2076–2100 future

time horizons. Therefore, the dam required further risk analysis study and dam safety modification in order to control this probable failure mode during the period of 2076–2100.

4. Conclusions

The purpose of this thesis is to predict the peak flow/flood that may load the reservoir in the future using a machine learning model and develop the HHC for the dam to assess the hydrologic risk for dam safety evaluation of the Kessem dam using the RMC-RFA software. Machine Learning models were used to simulate future stream flow and peak inflow hybrids with the SCS-CN model using the future LULC scenario and the climate projection under the RCP emission scenario. Based on an inflow-volume frequency analysis of Kessem Dam, the hydrological hazard at Kessem Dam was assessed using RMC-RFA software for three future time horizons (2022–2051, 2051–2075, and 2076–2100). However, the following conclusions were drawn from this study:

A novel approach to stream flow simulation based on recurrent neural networks is presented. It is one of the powerful ML predictive models. For this purpose, 70% of the flow data is trained on RNNs, including Bi-LSTM, LSTM, and GRU. Then, the remaining 30% of the data was used for performance evaluation. For each of the networks, the double hidden layer was used. The numbers of neurons in the hidden layers, the learning rate, and the number of iterations have a basic role in modeling accuracy, the optimal values of which were obtained using trial and error. Using the dropout function in the network structure can prevent network over fitting. To attain this purpose, all models were coded in Python 3.9 programming software within the Jupyter notebook by using different Python packages. The efficiency of the proposed predictive approach is evaluated for the simulation of daily inflow to the Kessem Dam reservoir in the Kessem watershed. Results of the study point to the better performance of Bi-LSTM compared to the other RNN architectures. The Bi-LSTM network performed the best and can estimate stream flow with fairly good accuracy, so it can be said that these networks can be used as an effective method of stream flow modeling and predict the peak flow for this study area.

The performance of the Bi-LSTM model to simulate stream flow at the dam location in the Kessem watershed for the baseline period (1990–2013) was acceptable, with Nash Sutcliffe Efficiency and Root Mean Square Error (NSE = 0.968 & RMSE = 3.873) for calibration and (NSE = 0.744 & RMSE = 17.547) for validation, and it outperformed other proposed ML models, so used it to predict future daily peak flows. The result was 467.72 m^3/s, 435.88 m^3/s, and 513.55 m^3/s of predicted daily peak flow during the periods of 2022–2050, 2051–2075, and 2076–2100, respectively.

The result of the HHC showed that 2,823.57 m^3/s and 935.21 m, 2,126.3 m^3/s and 934.18 m, and 11,491.1 m^3/s and 942.11 m peak inflow and peak reservoir water level during the periods of 2022–2050, 2051–2075, and 2076–2100, respectively, for 0.0001 APE. This means during the periods of 2022–2100 and 2051–2075, the peak discharge does not exceed the PMF and the overtopping does not occur in these periods of years. That means the dam passes through the PMF. The outcome of the semi-quantitative risk analysis carried out showed that for all peak flood potential loading, the results indicate that Kessem dam may potentially be overtopped by a flood with a return period of about 10,000 years during the period of

2076–2100. Because the coming peak discharge does not pass through a PMF for 2076–2100 future time horizons, it means the Kessem Dam does not meet Reclamation hydrologic hazard criteria for overtopping. Therefore, the dam required further risk analysis study regarding its consequences and damage, and how to modify dam safety in order to control this probable failure mode during the period of 2076–2100. Otherwise, the dam is safe within the period of 2022–2075. But all the critical upcoming peak flows pass through the dam spillway, which means that the existing spillway capacity is sufficient to surcharge the coming excess water without overtopping.

This study contributes scientific information regarding the future flood to Kessem dam reservoir and assesses its hazard on dam safety, which will be beneficial to take measurements to control floods during wet seasons, especially in August and September, to improve the dam safety and further the next level of risk assessment study.

Declarations

Acknowledgement

The authors would like to thank the Ethiopian Ministry of Water and Energy, Ethiopian National Meteorological Agency, Ethiopian Construction Works Cooperation and United States Geological Survey (USGS) for providing essential data for this study and Arba Minch University.

Funding

Not applicable

Competing interests

The authors declare no competing interests.

Ethics approval

We guarantee that the work described has not been submitted elsewhere for publication, and all the authors listed have agreed to submit the manuscript.

Consent to participate

The author agrees to participate in Theoretical and Applied Climatology

Consent for publication

The research is scientifically consented to be published.

Data Availability

The datasets generated during and/or analyzed during the current study are not publicly available due to the agreement between data provider organizations but are available from the corresponding author on reasonable request.

Code Availability

The code generated during the current study is available from the first author on reasonable request.

Author Contributions

Esayas Tesfaye Ergete: Conceptualization, Data curation, Methodology, Software, Code, Validation, Data analysis, writing-original draft.

Elias Gebeyehu Ayele: Conceptualization, Data curation, Investigation, Methodology, Supervision, Writing review and editing.

References

1. Adamo N, Al-Ansari N, Laue J, et al. (2017) Risk Management Concepts in Dam Safety Evaluation: Mosul Dam as a Case Study. Journal of Civil Engineering and Architecture 11: 635–652. https://doi.org/10.17265/1934-7359/2017.07.002
2. Adiel K, Qianli D, Gregory B Baecher, et al. (2015) *Systems Reliability of Flow Control in Dam Safety.* Paper presented at the International Conference on Applications of Statistics and Probability in Civil Engineering, Vancouver, Canada.
3. Assefa T (2018) Flood Risk Assessment in Ethiopia. Civil and Environmental Research 10(1): 35–40.
4. Bartles Michael, Brunner Gary, Fleming Matthew, et al. (2019) HEC-SSP Statistical Software Package User's Manual. USACE Hydrologic Engineering Center.
5. Getahun YS, Gebre SL (2015) Flood Hazard Assessment and Mapping of Flood Inundation Area of the Awash River Basin in Ethiopia using GIS and HEC-GeoRAS/HEC-RAS Model. Journal of Civil & Environmental Engineering 5(4): 1–12. https://doi.org/10.4172/2165-784X.1000179
6. Herrero A, Garrote J (2020) Flood Risk Analysis and Assessment,Applications and Uncertainties: A Bibliometric Review. Water 12(7): 1–24. https://doi.org/10.3390/w12072050
7. Hosseiny H, Nazari F, Smith V, et al. (2020). A Framework for Modeling Flood Depth Using a Hybrid of Hydraulics and Machine Learning.

8. Hunter J (2007) Matplotlib: A 2d Graphics Environment. Computing in Science & Engineering 9(3): 90–95. https://doi.org/10.1109/MCSE.2007.55
9. Jandora J, Riha J (2008) *The Failure of Embankment Dams due to Overtopping* (Aujeský František & Turland Roger, Trans.). Václav Houf
10. Khalaf M, Hussain A, Al-Jumeily D, et al. (2018) A Data Science Methodology Based on Machine Learning Algorithms for Flood Severity Prediction. IEEE Congress on Evolutionary Computation (CEC) 7(18). https://doi.org/10.1109/cec.2018.8477904
11. Kratzert F, Klotz D, Brenner C, et al. (2018) Rainfall–runoff modelling using Long Short-Term Memory (LSTM) networks. Hydrology and Earth System Sciences 22: 6005–6022. https://doi.org/10.5194/hess-22-6005-2018
12. Le X, Ho H, Lee G, et al. (2019) Application of Long Short-Term Memory (LSTM) Neural Network for Flood Forecasting. Water 11(7): 1387. https://doi.org/10.3390/w11071387
13. Mahmood R, Roger A, Hubbard K, et al. (2010) Impacts of land use/land cover change on climate and future research priorities. 91(1): 37–46.
14. Mcgrath S. (2000). *To Study International Practice and Use of Risk Assessment in Dam Management*. Retrieved from
15. Mich L (2020) Artificial Intelligence and Machine Learning. Handbook of e-Tourism: 1–21. https://doi.org/10.1007/978-3-030-05324-6_25-1
16. Mo C, Mo G, Yang Q, et al. (2018) A quantitative model for danger degree evaluation of staged operation of earth dam reservoir in flood season and its application. Water Science and Engineering journal 11(1): 81–87. https://doi.org/10.1016/j.wse.2017.07.001
17. OCHA. (2020). *Ethiopia: Floods United Nations Ofices for the Coordination of Humanitarian Affairs, Update No.3*. Retrieved from
18. Raghunath H (2006) *Hydrology Principles,Analysis and Design* (Second ed.). New Delhi: New Age International (P) Ltd
19. Rao A, Hamed K (2000) *Flood Frequency Analysis* (First ed.). CRC Press, Boca Raton
20. Roberts W, Williams G, Jackson E, et al. (2018) Hydrostats: A Python package for characterizing errors between observed and predicted time series. Hydrology 5(4). https://doi.org/10.3390/hydrology5040066
21. Rossum G. (1995). *Python Tuterial (Report CS-R9526). Retrieved from Amsterdam, the Netherlands*. Retrieved from Amsterdam, the Netherlands:
22. Sharma R, Ali K (2013) *Case histories of earthen dam failures.* Paper presented at the International Conferenceon Case Histories in Geotechnical Engineering, Missouri University of Science and Technology.
23. Shoaib Muhammad, Shamseldin Asaad Y, Melville Bruce W (2014) Comparative study of different wavelet based neural network models for rainfall–runoff modeling. Journal of Hydrology 515: 47–58.
24. Shumie M (2019) Evaluation of Potential Reservoir Deficiency Due to Climate Change, Kesem Kebena Dam, Ethiopia. Journal of Environmental Geography 12(1–2): 33–40. https://doi.org/10.2478/jengeo-

2019-0004

25. Sivapalan M, Blöschl G, Merz R, et al. (2005) Linking flood frequency to long-term water balance: Incorporating effects of seasonality. Water Resources Research 41(6). https://doi.org/10.1029/2004WR003439
26. Subramanya K (2008) *Engineering Hydrology* (Third ed.). Tata McGraw-Hill Publishing Company Limited, NEW DELHI
27. Vo N, Gourbesville P, Vu M, et al. (2015) A deterministic hydrological approach to estimate climate change impact on river flow: Vu Gia–Thu Bon catchment, Vietnam. Journal of Hydro-environment Research 11: 59–74. https://doi.org/10.1016/j.jher.2015.11.001
28. Wilby R, Dawson C (2007) *SDSM 4.2-A decision support tool for the assessment of regional climate change impacts. User manual*
29. Zhang Q, Zhang L, She D, et al. (2021) Automatic procedure for selecting flood events and identifying flood characteristics from daily streamflow data. Environmental Modelling and Software 145: 1–12. https://doi.org/10.1016/j.envsoft.2021.105180

Figures

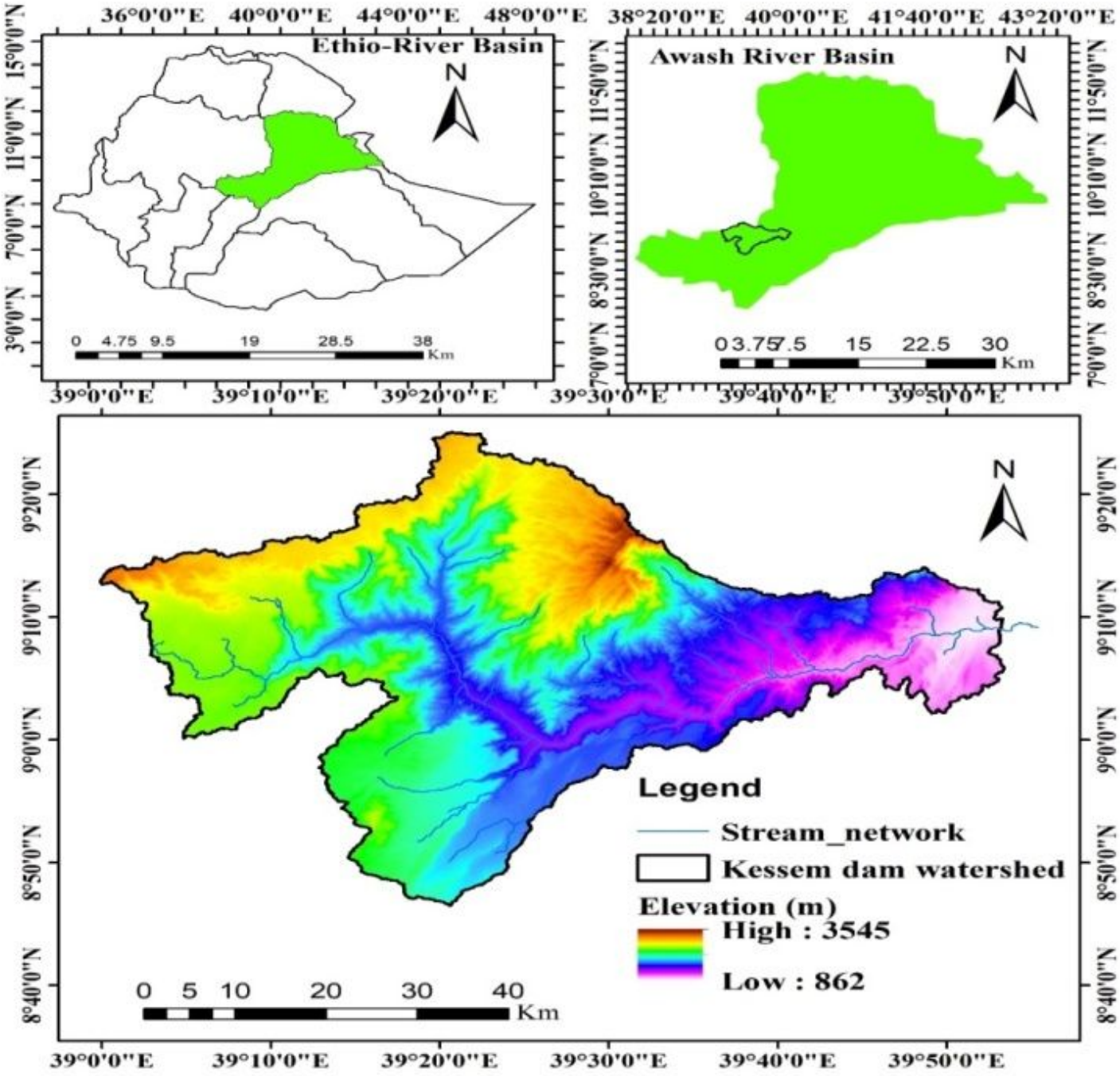

Figure 1

Topographical map of the study area

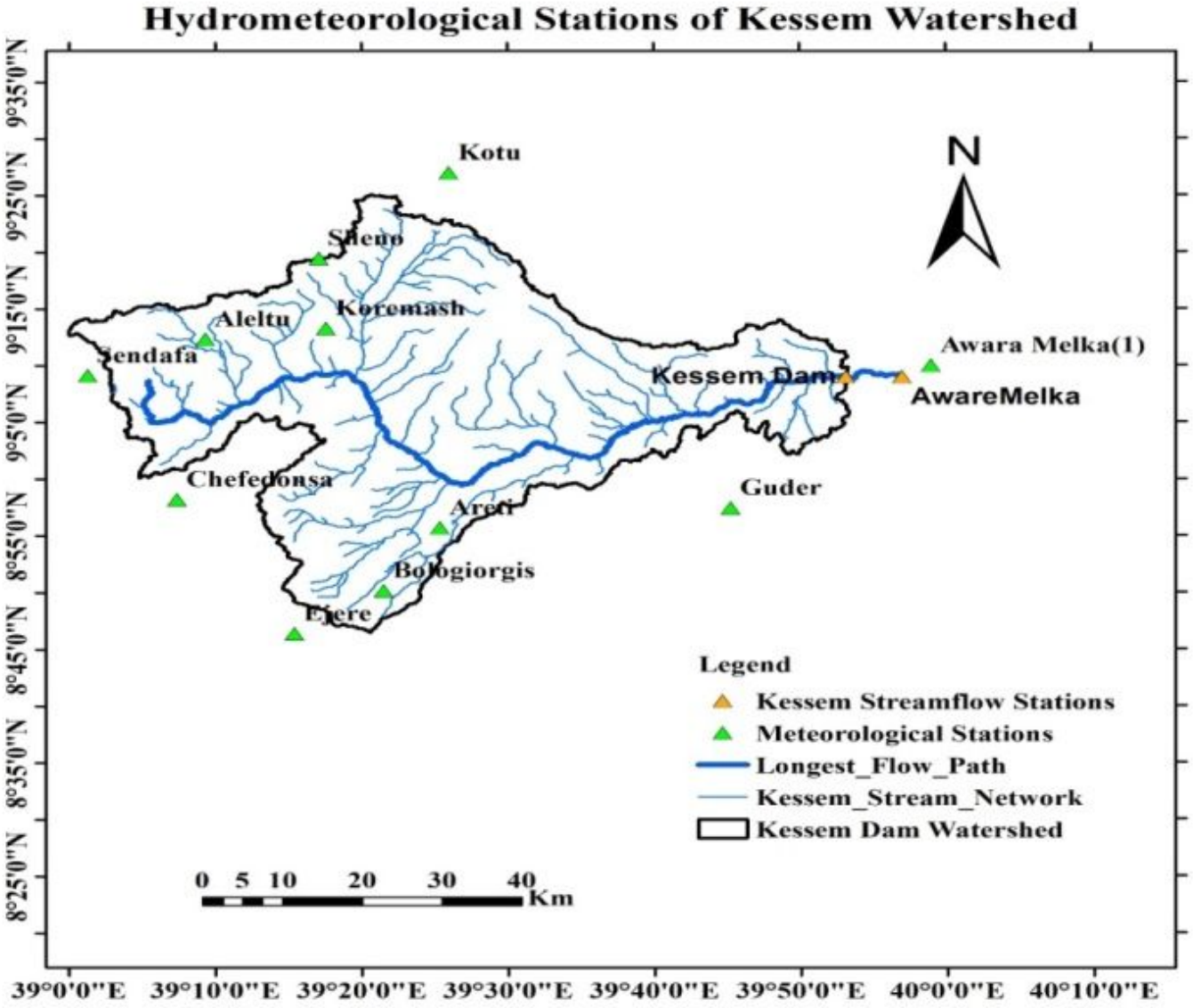

Figure 2

Hydro-metrological stations

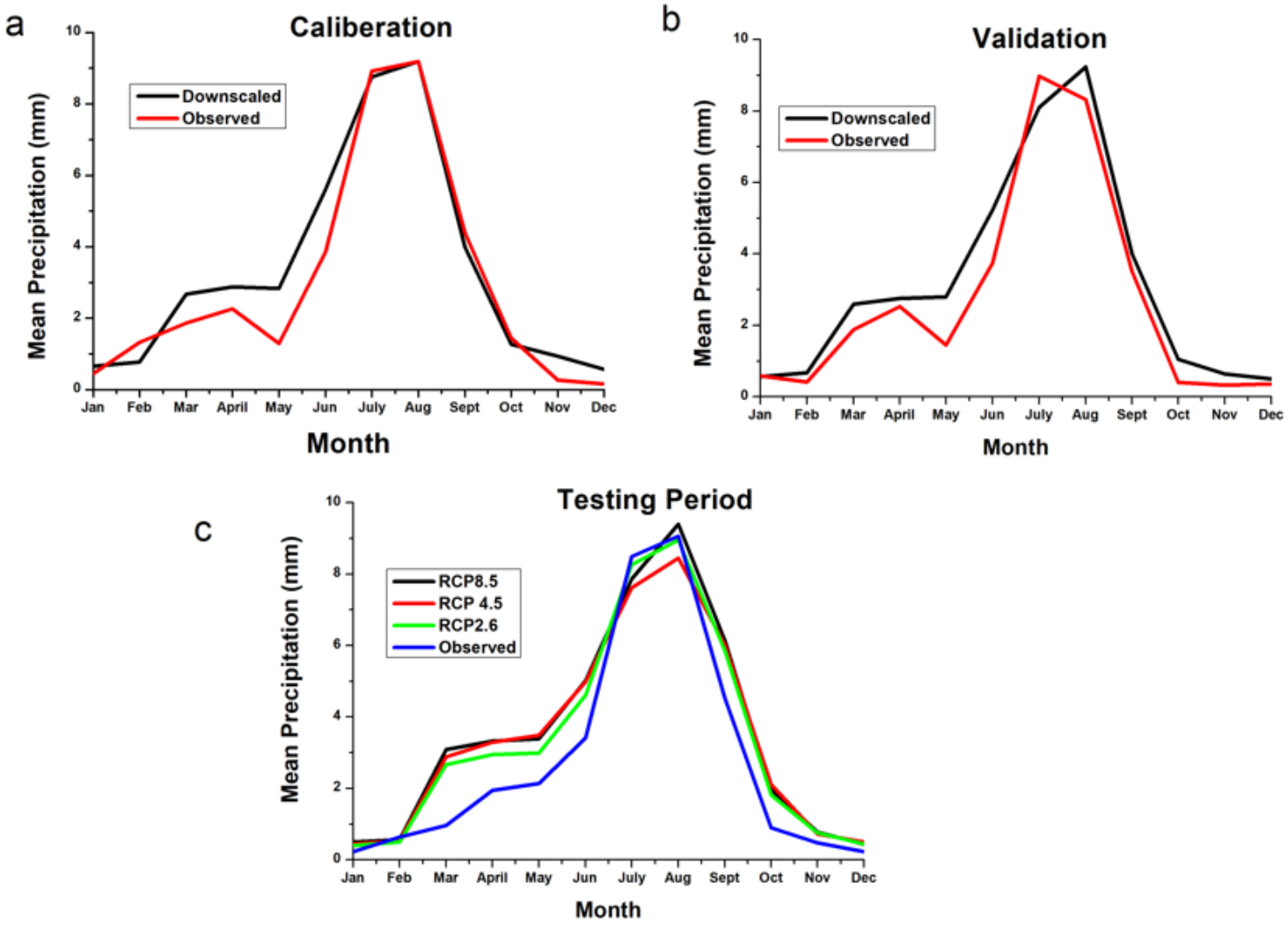

Figure 3

Downscaled vs observed mean precipitation of Kessem watershed; a) for model calibration period (1988-1999), b) for validation period (2000-2005), and c) for testing period (2006-2018)

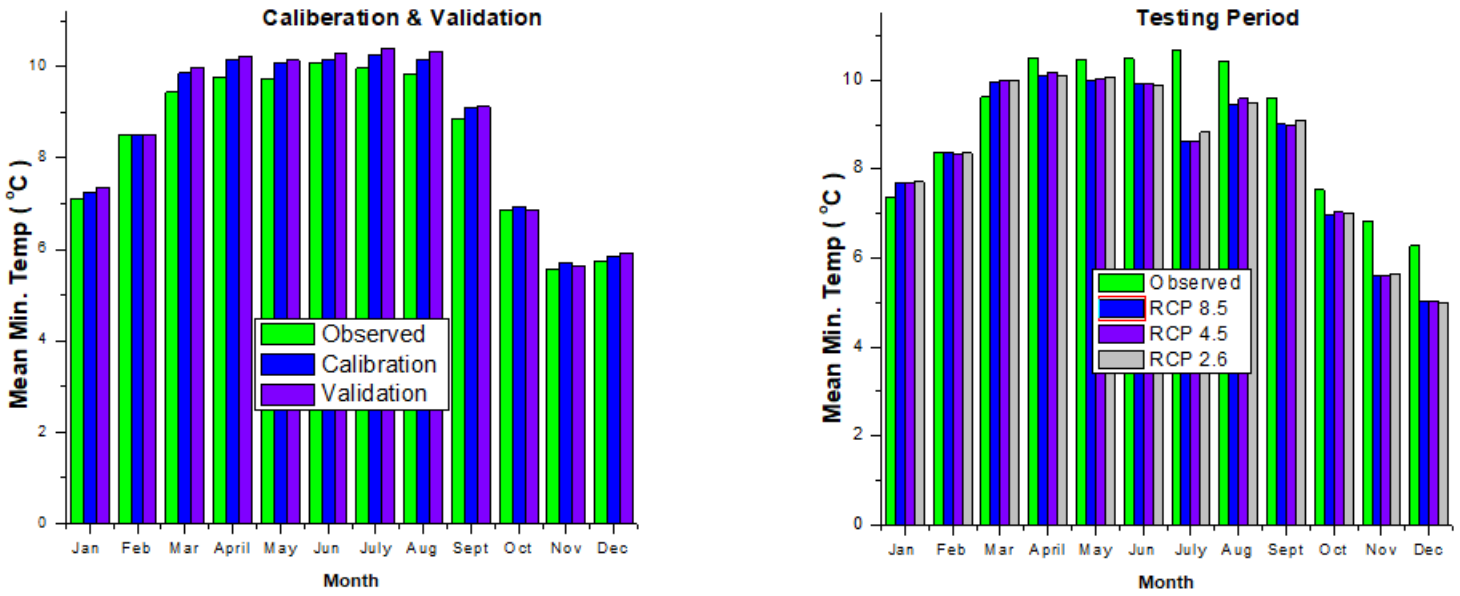

Figure 4

Downscaled vs observed mean minimum temperature of Kessem watershed for model calibration period (1988-1999), validation period (2000-2005), and testing period (2006-2018)

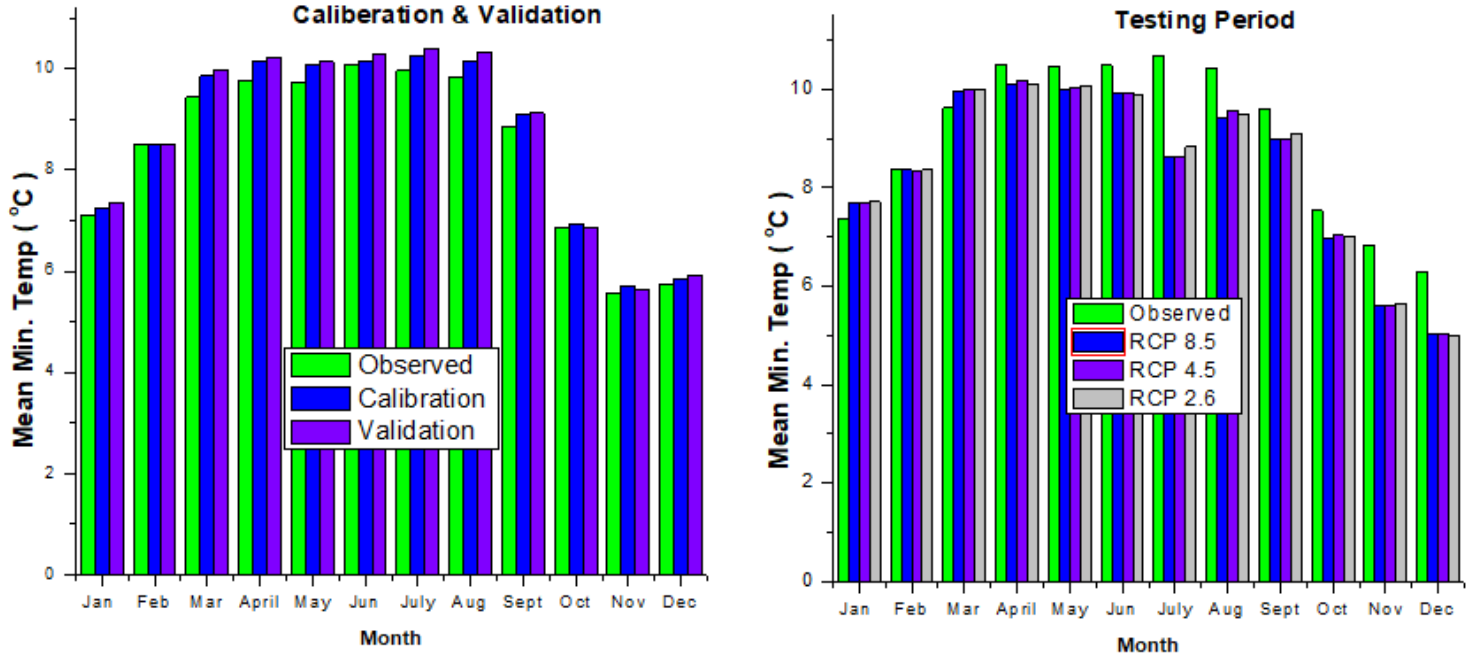

Figure 5

Downscaled vs observed mean maximum temperature of Kessem watershed; for model calibration period (1988-1999), validation period (2000-2005), and testing period (2006-2018)

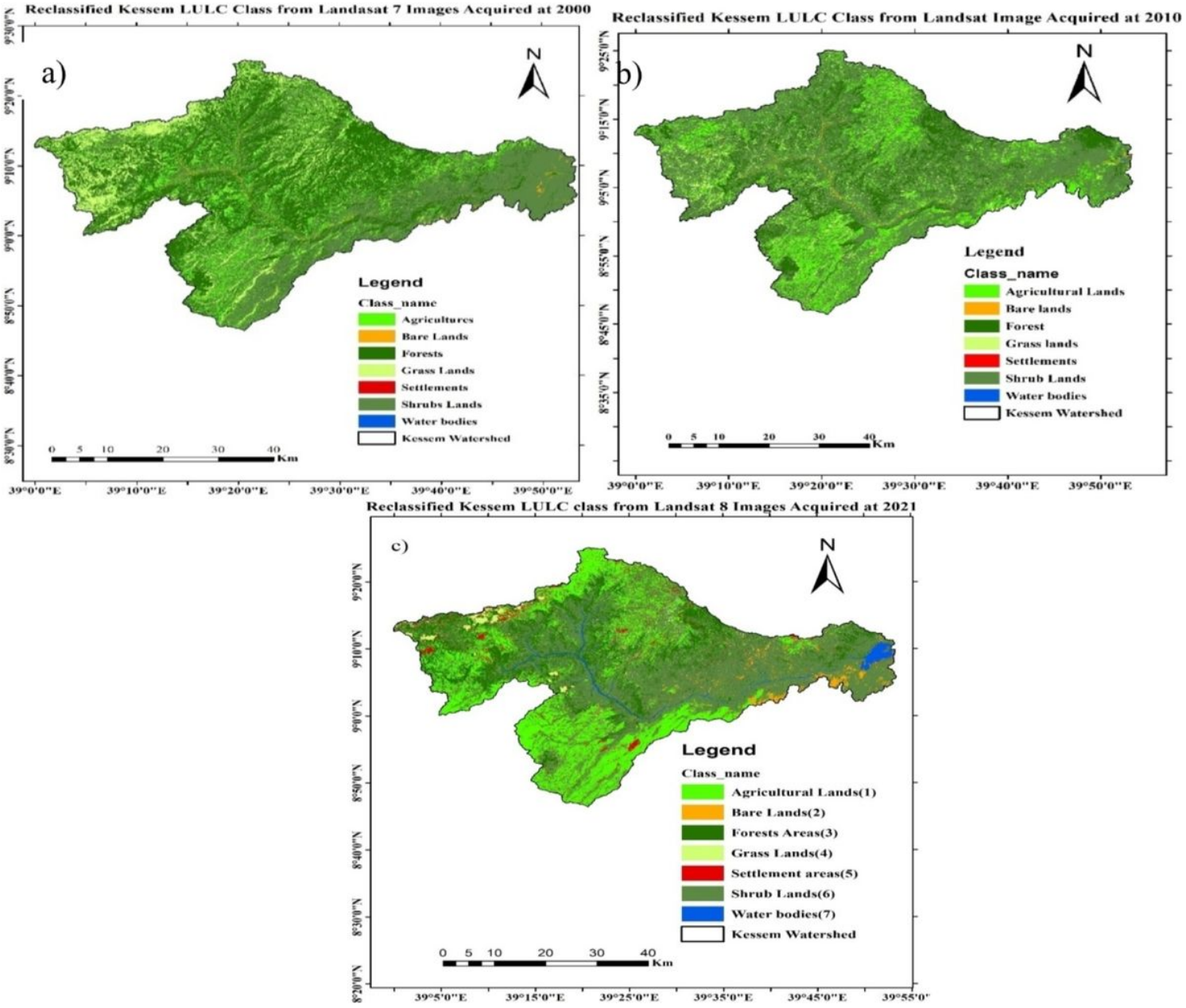

Figure 6

Reclassified Kessem watershed LULC class based on used Landsat Image acquired at, a) 2000, b) 2010, and c) 2021 or present day

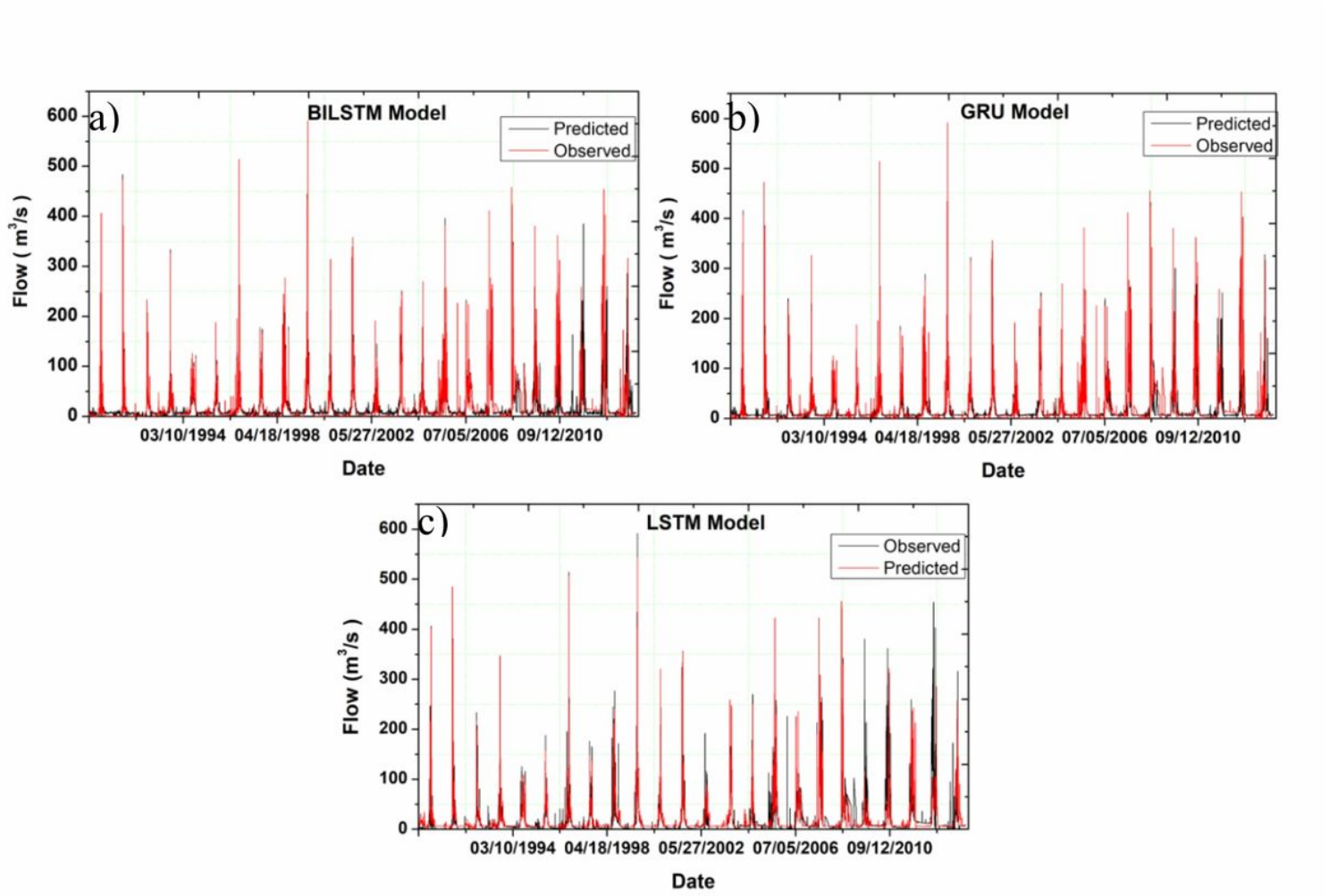

Figure 7

Visualized the performance of predictive models results for training and testing period; a) Bi-LSTM Model, b) LSTM model, and c) GRU model

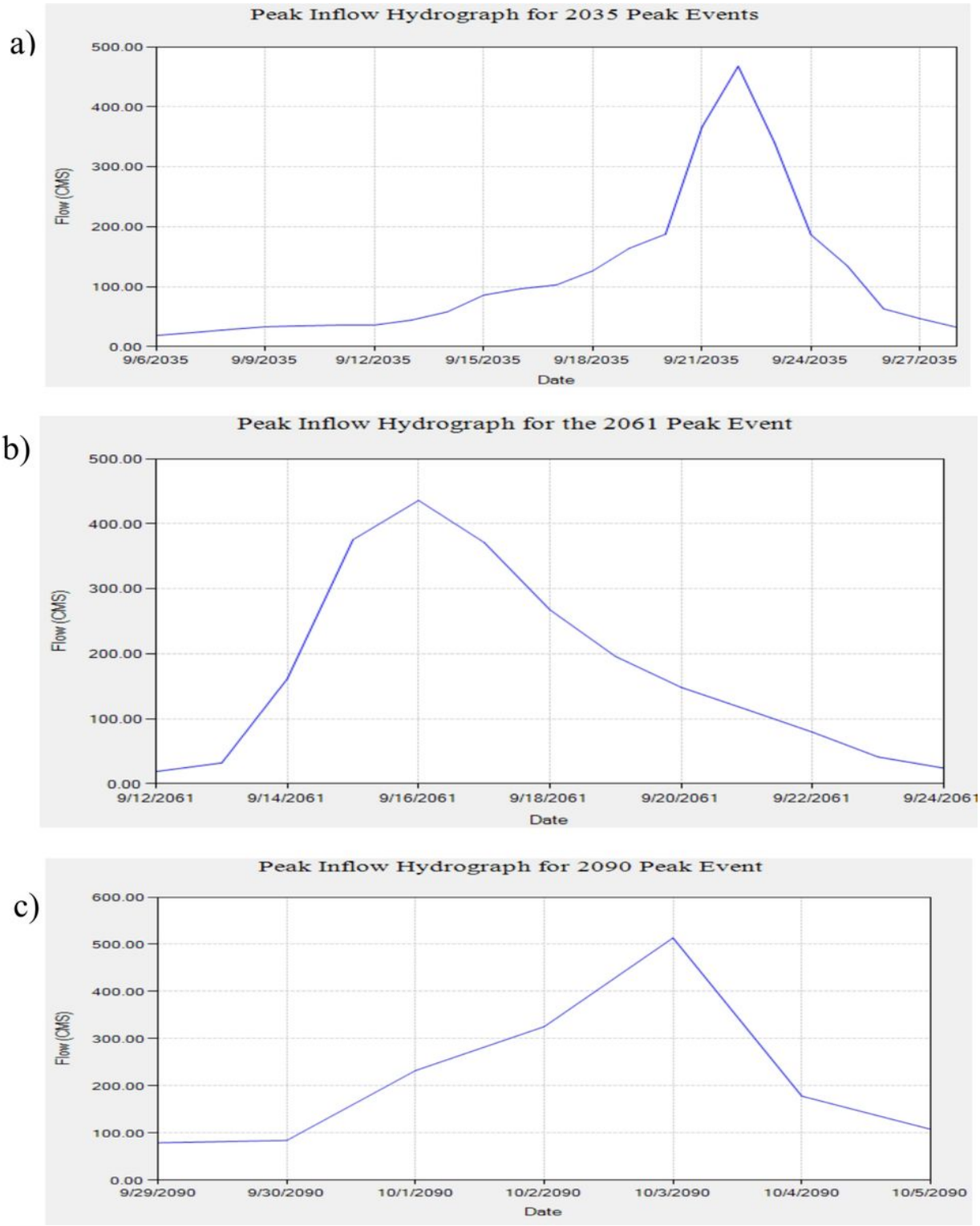

Figure 8

Peak Inflow Hydrograph a) 2035 flood event from during 2022-2050, b) 2061 flood event from during 2051-2075, and c) 2090 flood event from during 2076-2100

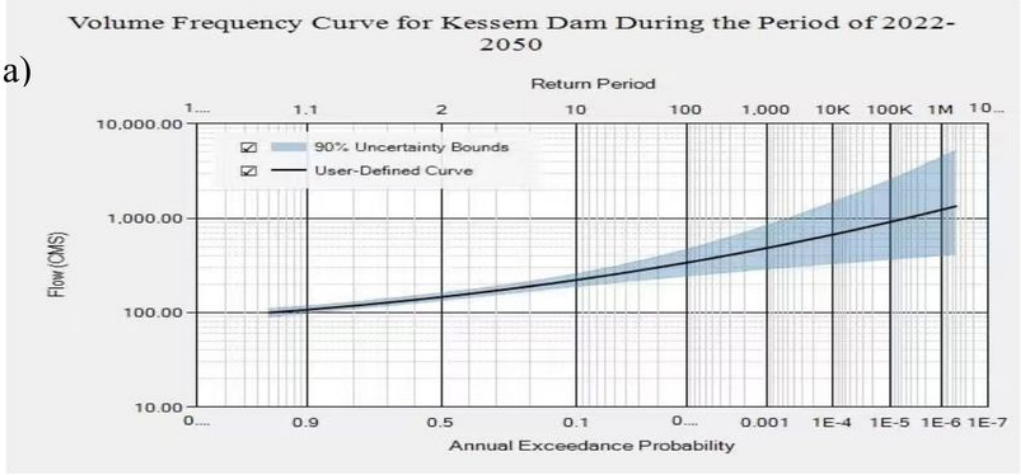

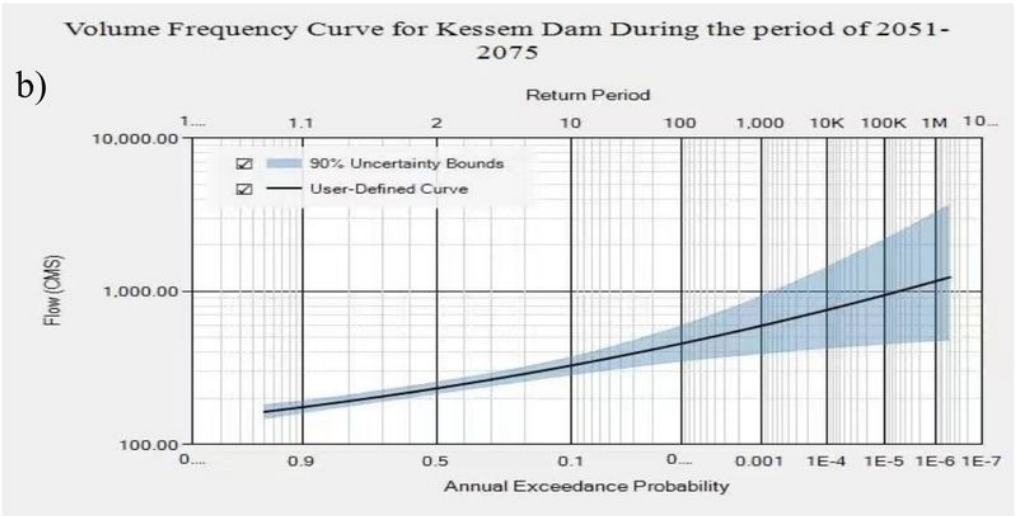

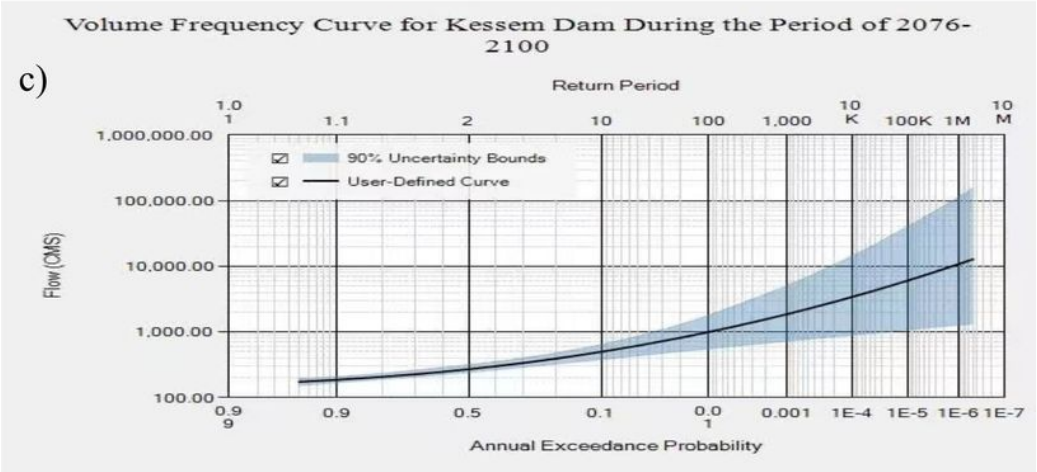

Figure 9

The PMF hydrograph of Kessem dam

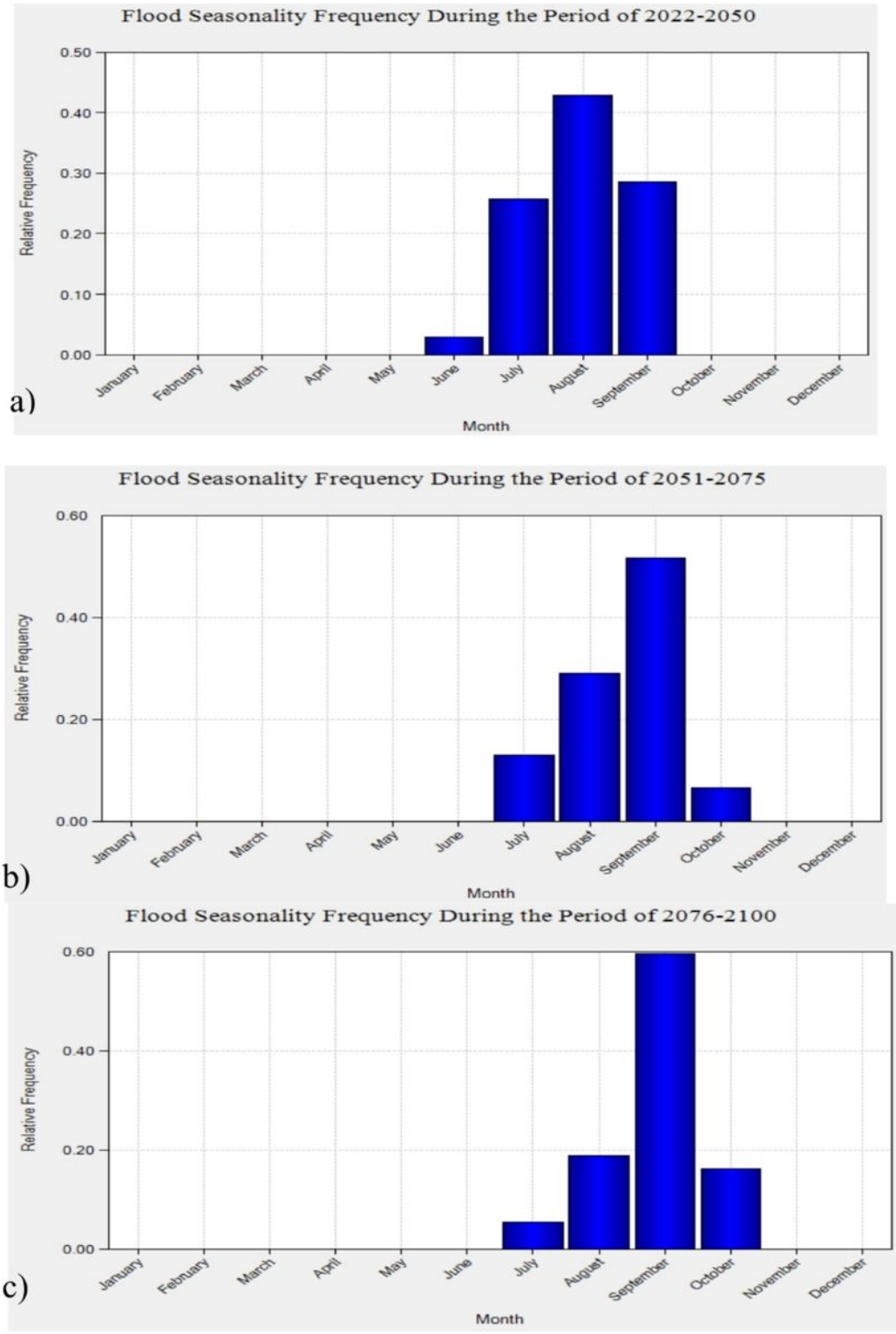

Figure 10

Volume Frequency Curve for Kessem Dam; a) During the period of 2022-2050, b) of 2051-2075 and c) of 2076-2100

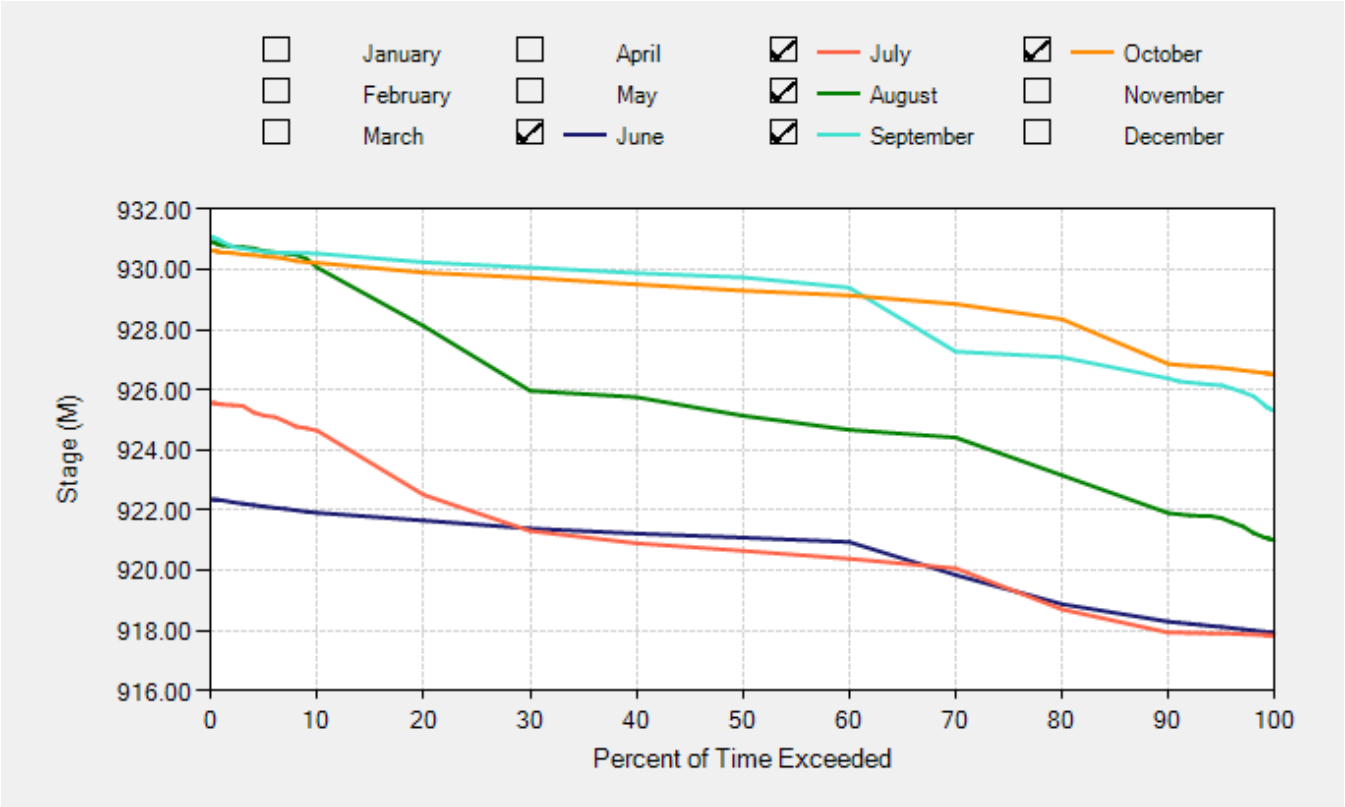

Figure 11

Flood Seasonality Analysis for Kessem Dam; a) in period of 2022-2050, b) in period of 2051-2075 and c) in the period of 2076-2100

a)

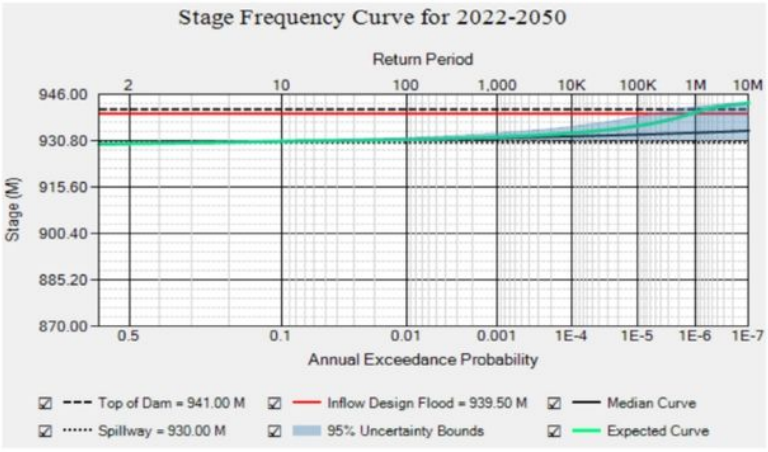

b)

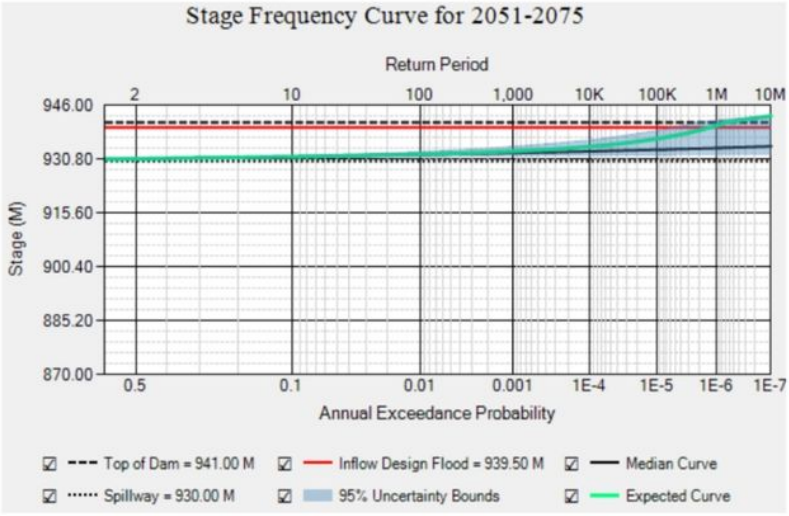

c)

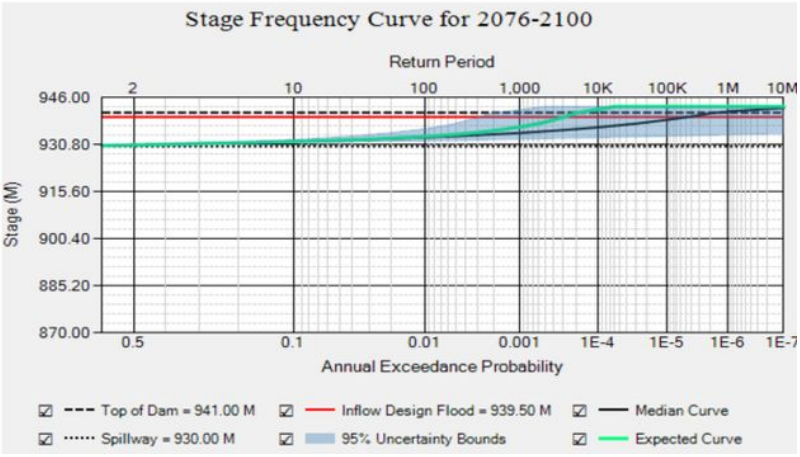

Figure 12

Reservoir starting-stage duration analysis for Kessem dam in flood season

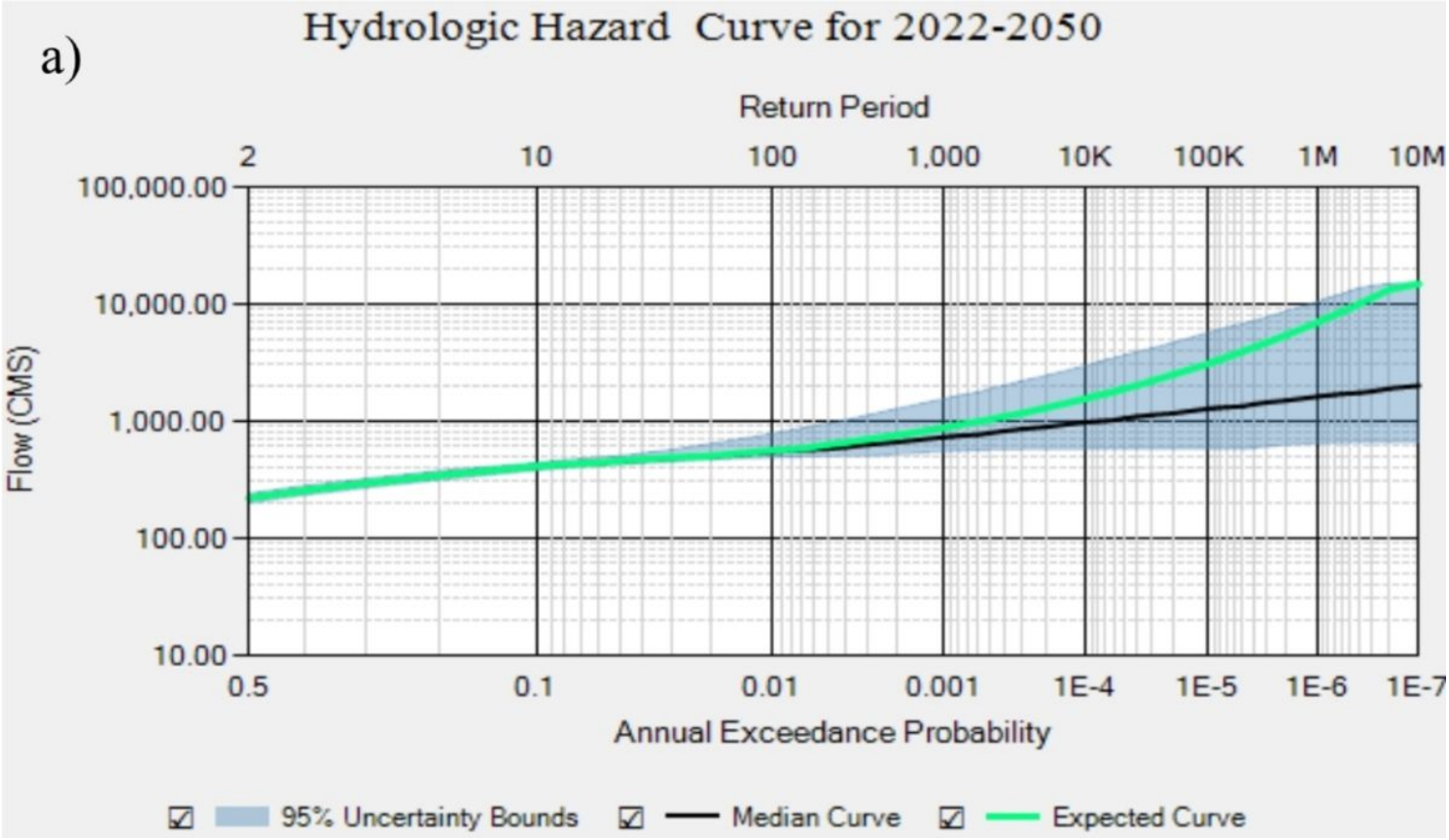

Figure 13

Stage Frequency Curve for Kessem Dam during the period of: a) 2022 to 2050, b) 2051-2075, c) 2076-2100

b)

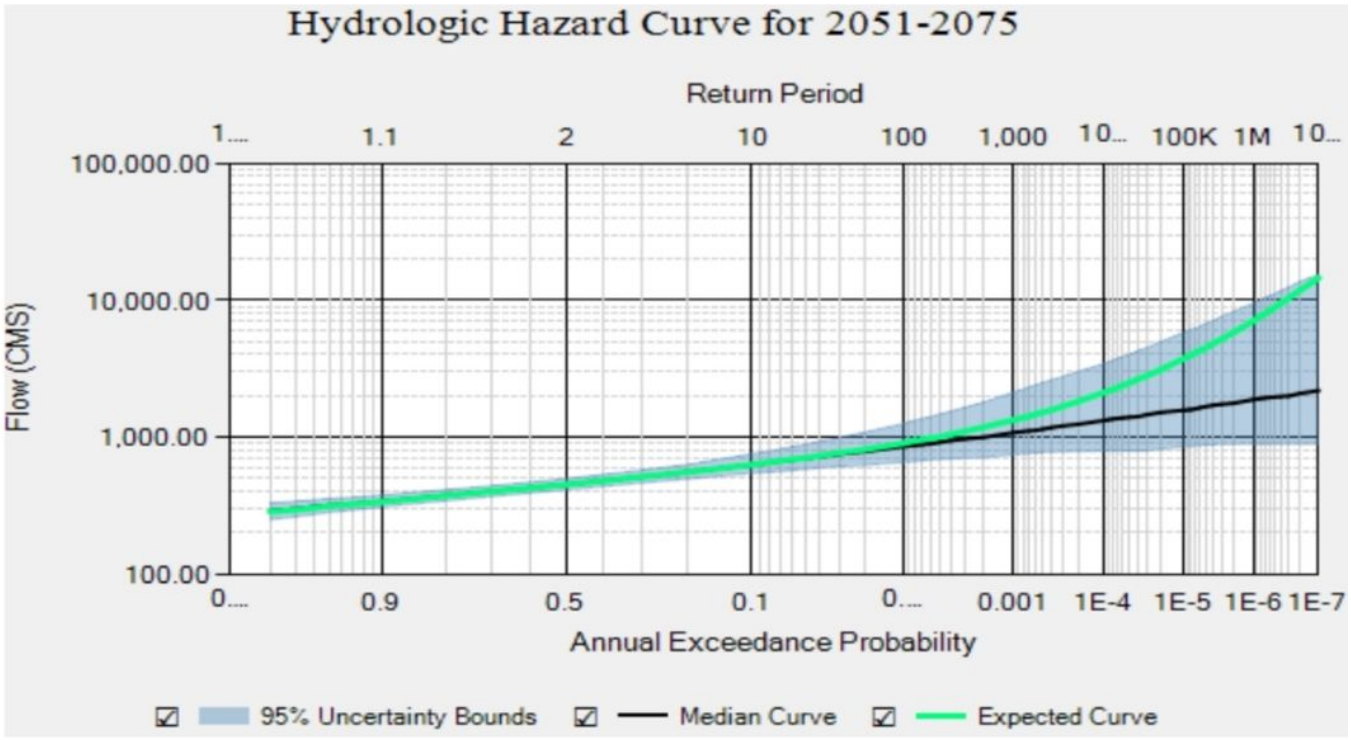

c)

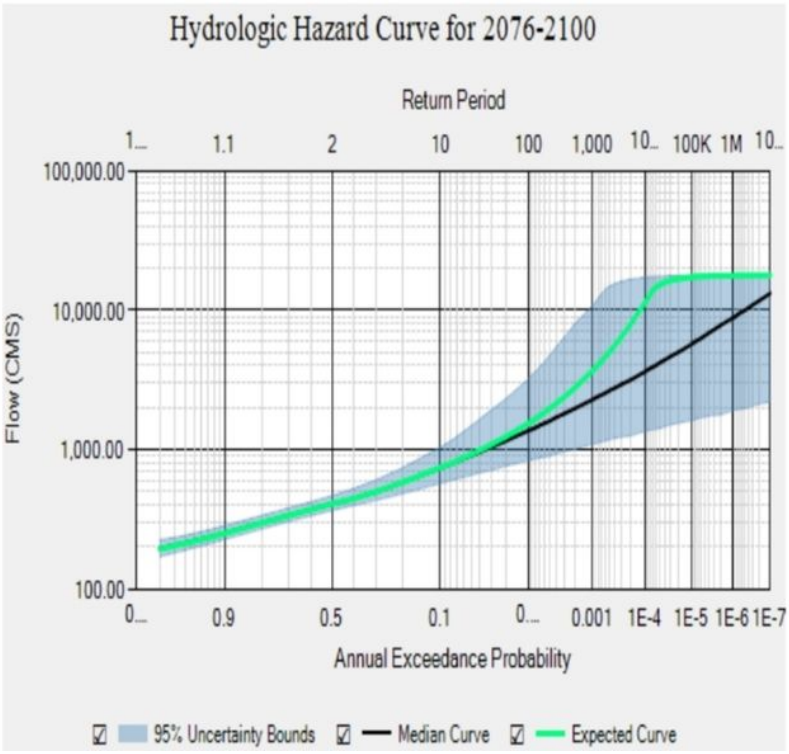

Figure 14

Hydrologic Hazard curve for Kessem dam during the period of: a) 2022-2050, b) 2051-2075, and c) 2076-2100